THE INTRINSIC SUBMICRON ZNO THIN FILMS PREPARED BY REACTIVE MAGNETRON SPUTTERING

REMES Zdenek*[1,2], STUCHLIK Jiri[1], PURKRT Adam[1], CHANG Yu-Ying[1,2], JIRASEK Vit[1], STENCLOVA Pavla[1], PRAJZLER Vaclav[3], NEKVINDOVA Pavla[4]

[1]*Institute of Physics Institute of Physics CAS, Prague, Czech Republic, EU*
[2]*Faculty of Biomedical Engineering CTU in Prague, Kladno, Czech Republic, EU*
[3]*Faculty of Electrical Engineering CTU in Prague, Prague, Czech Republic, EU*
[4]*Department of Inorganic Chemistry UCT, Prague, Czech Republic, EU*
*remes@fzu.cz

Abstract

The DC reactive magnetron sputtering of metallic target in oxide atmosphere is a simple method of depositing the intrinsic (undoped) nanocrystalline layers of metal oxides. We have optimized the deposition of the intrinsic ZnO thin films with submicron thickness 50–500 nm on fused silica glass substrates and investigated the localized defect states below the optical absorption edge down to 0.01 % using photothermal deflection spectroscopy from UV to IR. We have shown that the defect density, the optical absorptance and the related optical attenuation in planar waveguides can be significantly reduced by annealing in air at 400 °C.

Keywords: ZnO, reactive magnetron sputtering, plasma treatment, photothermal deflection spectroscopy, optical spectroscopy

1. INTRODUCTION

ZnO is classified as a semiconductor group II-VI, whose covalence is on the boundary between ionic and covalent semiconductors [1]. It is nowadays a subject of a large attention due to the interesting physical properties such as wide direct band gap, high refractive index, high thermal conductivity and large exciton binding energy [2]. These properties uncover a wide range of optical, electrical and magnetic devices and appliances, i.e. in solar cells [3], electroluminescence diodes [4], surface acoustic devises [5], photodetectors or biosensors [6]. ZnO layers doped with magnetic metals, such as Mn, Co and Ni have recently attracted interests as diluted magnetic semiconductors for spintronic device applications [7]. There has been also theoretically predicted and experimentally confirmed the room temperature ferromagnetism induced by non-magnetic ionic dopants [8]. First-principles studies have provided an insight into the atomic and electronic structures of native point defects and impurities and defect-induced properties of ZnO [9]. They predict that the O vacancy is a very deep donor and cannot be a major source of carrier electrons. The Zn interstitial and anti-site defects are shallow donors, but these defects are unlikely to form at a high concentration in n-type ZnO under thermal equilibrium due to high forming energy. Important extrinsic defect can be hydrogen, presumably a shallow donor [10].

The high optical transparency and the high refractive index contrast opens the way to the implementation of the ultra-small bending radius, ultra-compact, ultra-dense integrated photonic structures operating in extreme conditions providing an outstanding platform for the development of new photonic structures in wide spectral range [11]. However, the requirements for optical quality of optical waveguides are very challenging. The optical absorption and the optical scattering at grain boundaries are the critical issue in photonic applications such as multimode interference demultiplexer [12]. The association between the optical absorptance inside the band gap on one side, and the impurities and defect perturbations inside the atomic structure of the ZnO lattice on the other, is far from satisfactory. The goal of this paper is to show the effect on thermal annealing

of the nominally undoped ZnO thin films with the submicron thickness prepared by reactive magnetron sputtering of metal target on the concentration of the localized defect states in electron energy gap.

2. EXPERIMENTAL

2.1. Reactive magnetron sputtering

In the magnetron sputtering process the plate target (cathode) is bombarded by the positively charged energetic Ar+ ions generated in glow discharge plasma. The bombardment process causes the removal, i.e., sputtering, of target atoms, which then diffuse towards a substrate where they condense in the form of the thin film in a process called physical vapor deposition. Secondary electrons are also emitted from the target surface as a result of the ion bombardment, and these electrons together with magnetic field play an important role in maintaining the cold plasma [13, 14].

Figure 1 Reactive magnetron sputtering equipment

Reactive magnetron sputtering has been done in the stainless steel vacuum chamber using Zn target with purity 99.9 %, diameter 60 mm, sputtered zone diameter 45 mm, distance between target and sample holder 75 mm, see **Figure 1**. The residual pressure (vacuum) was 0.01 Pa, magnetic field is induced electromagnetically by current 4.5 A. The target was sputtered in the reactive mixture of argon (purity 99.999 %) and oxygen (purity 99.95 %) under flow rate 2.0 and 0.5 sccm and the pressure 1 Pa. The voltage at the target was kept constant 400 V and the current 0.13 A. The temperature of the resistively heated substrate holder stage was regulated from 100 to 450 °C.

2.2. Optical spectroscopy

Unlike the transmittance and reflectance spectroscopy, the photothermal deflection spectroscopy (PDS) measures directly the optical absorption of thin films with high sensitivity of four orders of magnitude [15]. Our PDS setup uses the 150 W Xe lamp, the monochromator equipped with three gratings blazed at 300, 750, 1250 nm and a chopper operating at low frequency a light source. The heat absorbed in the sample generates the periodical thermal waves in the medium surrounding the sample causing the periodical deflection of the

laser beam parallel to the sample surface. The amplitude of the deflection normalized on the black sample spectra gives the optical absorption of thin film. The monochromatic light is partly deflected by the beamsplitter into the compound detector based on the integrating sphere equipped with Si and InGaAs photodiodes to monitor the light intensity in the broad spectral range from ultraviolet to infrared region 250–1700 nm. The compound detectors are also placed in front and behind the sample to detect the reflected and transmitted light, whereas the optical absorptance is detected by the position detector monitoring the laser beam deflection. The signal from the detectors is coupled via the multiplexer to the current preamplifier and a lock-in amplifier referenced to the chopper frequency.

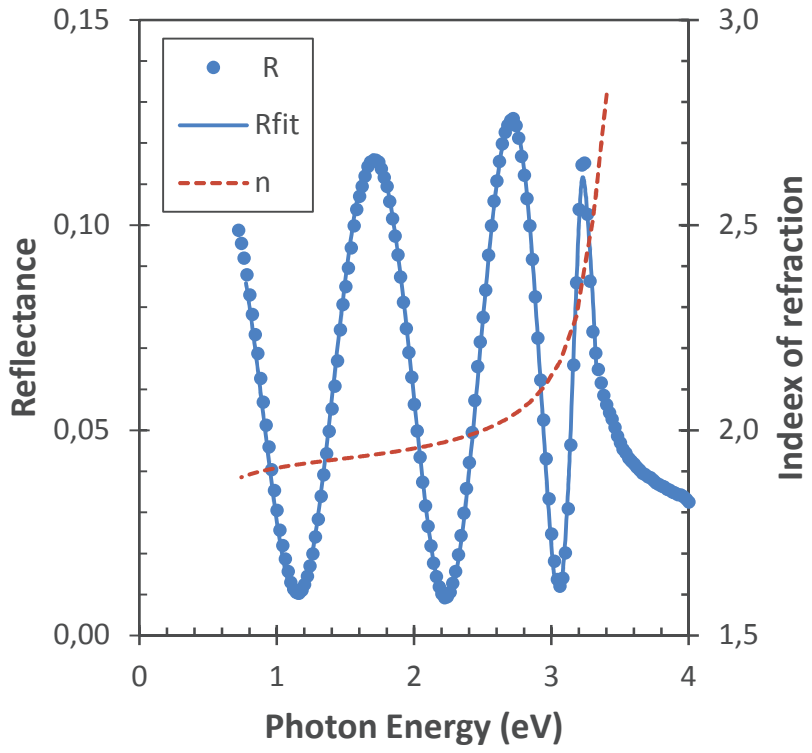

Figure 2 The measured (R) and fitted (Rfit) reflectance spectra of 270 nm thick intrinsic ZnO layer compared to the index of refraction dispersion spectra (*n*)

3. RESULTS AND DISCUSSION

The reflectance spectrum of the thin intrinsic ZnO layer shows the interference fringes up to the optical absorption edge in near UV region at 3.3 eV, see **Figure 2**. To estimate the film thickness and the index of refraction we fitted the reflectance spectrum in non-absorbing region using mixed Lorentz oscillator and Drude dielectric function ε_1 (Eq. 1) where ε_∞ is the high frequency lattice dielectric constant, A the amplitude (strength) of the Lorentz oscillator, E_c the center energy of the Lorentz oscillator, E_v the vibration energy (broadening) of the Lorentz oscillator, E_p the plasma energy related to free electron density, charge and the effective mass and E_d the damping energy related to free electron collisions [16].

$$\varepsilon_1(E) = \varepsilon_\infty \left(1 + \frac{A^2}{E_c^2 - E(E - E_v)} - \frac{E_p^2}{E(E + iE_d)} \right) \tag{1}$$

$$(1 - f_0)\frac{\varepsilon_1 - \varepsilon_2}{\varepsilon_1 + 2\varepsilon_2} + f_0 \frac{\varepsilon_0 - \varepsilon_2}{\varepsilon_0 + 2\varepsilon_2} = 0 \tag{2}$$

To improve the fit quality, we extended our model by two layers system using the effective medium approximation (EMA). The first (bottom) layer represents ZnO with the thickness d_1 while the second (top) layer with thickness d_2 is a mixture of ZnO and voids with the volume fraction f_0. The dielectric function of the second layer ε_2 (Eq. 2) is calculated from the dielectric function of the first layer ε_1 and the surrounding medium ε_0 using the self-consistent Bruggeman model [17].

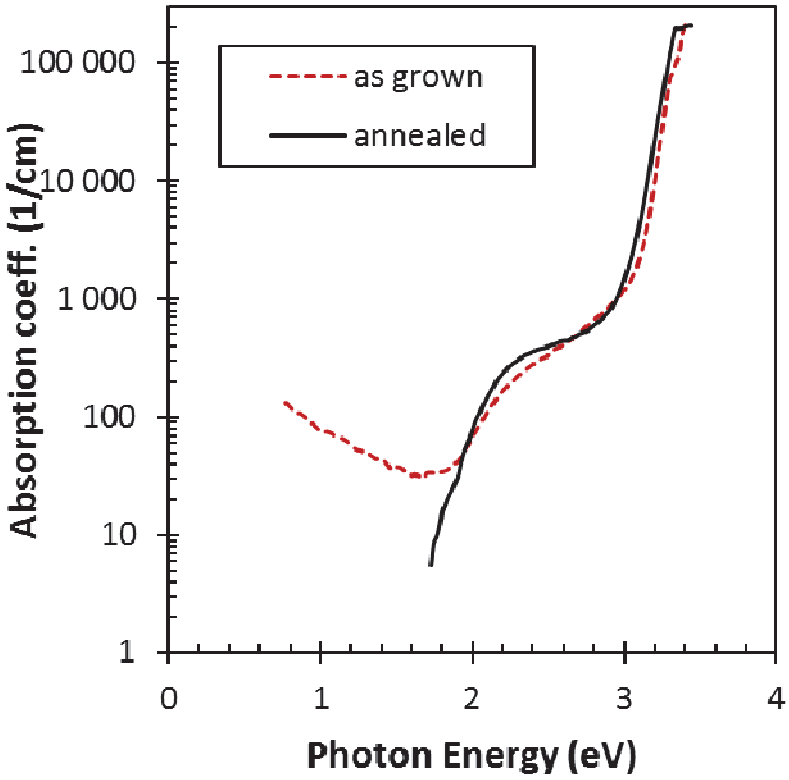

Figure 3 The optical absorption coefficient calculated independently at each wavelength from the absorptance spectra of the as grown ZnO layer before and after anneling in air at 400°C

The optical absorption coefficient is calculated in the two layer EMA model independently at each wavelength from the absorptance spectra using the dispersion spectra of the index of refraction calculated and the film thickness calculated from the reflectance spectra, see **Figure 3**. The direct band gap optical absorption edge is clearly observed at 3.3 eV as well as the defect related optical absorption below the absorption edge and the free carrier infrared absorption in the case of as grown layer that disappeared after annealing [18].

To estimate the role of the optical absorption on light attenuation in the ZnO/glass planar optical waveguide (PWG), we applied the 2D geometry finite-element method (FEM) using COMSOL Multiphysics® Software [19]. Prior to solving for the electromagnetic field in the PWG, mode analysis was done on both ports in order to calculate the effective mode index and corresponding out-of-plane wavenumber. Then, the electromagnetic field propagation was solved for the fundamental TE0 mode. Attenuation of the optical signal in the waveguide was calculated from the 21 component of the S-matrix (provided by FEM software). The calculated optical attenuations for selected wavelengths are summarized in **Table 1** where the values of real and imaginary parts of refractive index of ZnO were taken from reflectance & absorptance measurements except the k values for annealed sample at 0.8 eV, where the hypothetical value 1 cm^{-1} of the optical absorption coefficient was also used for comparison.

Table 1 The calculated optical attenuation *OA* for selected photon energies (*En*), wavelength (λ), absorp. coeff. α, the real (*n*) and imaginary (*k*) parts of the index of refraction. Values marketed * are hypothetical for comparison

	En (eV)	λ (nm)	*n*	*α(cm⁻¹)*	*k*	*OA* (dB/cm)
as grown	0.80	1550	1.84	139	1.72E-3	386
	0.93	1330	1.89	116	1.23E-3	379
	1.38	901	1.90	78	5.59E-4	312
	1.96	633	1.93	130	6.49E-4	530
annealed	0.8	1550	1.84	8	1.00E-4	5
				1*	1.00E-5*	0.5

The optical absorption in the visible region 2–3 eV is dominated by the deep defects that cannot be suppressed by temperature annealing. Therefore the optical attenuation is too high for applications in optical waveguides. The nominally undoped as grown ZnO exhibits the characteristic shape of the free carrier optical absorption in the infrared spectral region at photon energies below 2 eV and the high calculated optical attenuation in planar waveguide. On the other hand the infrared optical absorption coefficient of annealed sample was below the detection limit 10 cm^{-1}. Our calculations for hypothetical value 1 cm^{-1} show that in this case the optical absorption coefficient will be sufficiently low to drop the optical attenuation below 1 dB/cm.

4. CONCLUSION

We have optimized the deposition of the intrinsic ZnO thin films with the sub-micron thickness by the DC reactive magnetron sputtering of metallic target in oxide atmosphere and investigated the localized defect states below the optical absorption edge in a broad spectral range from near UV to near IR. We have shown that the optical absorption and related optical attenuation can be significantly reduced in the infrared region by annealing in air. However, the association between the electron states inside the band gap, the impurities and the defect perturbations inside the atomic structure of the ZnO lattice is not yet fully understood, which may be an obstacle when trying to use ZnO in applications such as planar waveguides. Therefore, the information on intrinsic defects based on the first principles calculations and further basic research is needed.

ACKNOWLEDGEMENTS

This work was supported by the project 16-10429J of the Czech Science Foundation and the project KONNECT-007 of the Czech Academy of Sciences.

REFERENCES

[1] KOŁODZIEJCZAK-RADZIMSKA, A., JESIONOWSKI, T. Zinc Oxide-From Synthesis to Application: A Review. *Materials*. 2014. Vol. 7, no. 4, pp. 2833-2881.

[2] JANOTTI, A., VAN DE WALLE, Ch. G. Fundamentals of zinc oxide as a semiconductor. *Reports on Progress in Physics*. 2009. Vol. 72, no. 12, p. 126501.

[3] VANECEK, M., BABCHENKO, O., PURKRT, A., HOLOVSKY, J., NEYKOVA, N., PORUBA, A., REMES, Z., MEIER, J., KROLL, U. Nanostructured three-dimensional thin film silicon solar cells with very high efficiency potential. *Applied Physics Letters*. 2011. Vol. 98, no. 16, p. 163503

[4] HSIEH, Y.-P, CHEN, H.-Y., LIN, M.-Z., SHIU, S.-Ch., HOFMANN, M., CHERN, M.-Y., JIA, X., YANG, Y.-J., CHANG, H.-J., HUANG, H.-M., TSENG, S.-Ch., CHEN, L.-Ch., CHEN, K.-H., LIN, Ch.-F., LIANG, Ch.-T., CHEN, Y.-F. Electroluminescence from ZnO/Si-Nanotips Light-Emitting Diodes. *Nano Letters*. 13 May 2009. Vol. 9, no. 5, pp. 1839-1843.

[5] WANG, W.-Sh., WU, T.-T., CHOU, T.-H. CHEN, Y.-Y. A ZnO nanorod-based SAW oscillator system for ultraviolet detection. *Nanotechnology*. 2009. Vol. 20, no. 13, p. 135503.

[6] SINGH, R. Ch., SINGH, O., SINGH, M. Pal, CHANDI, P. S. Synthesis of zinc oxide nanorods and nanoparticles by chemical route and their comparative study as ethanol sensors. *Sensors and Actuators B: Chemical*. 2008. Vol. 135, no. 1, pp. 352-357.

[7] PEARTON, S. J., ABERNATHY, C. R., OVERBERG, M. E., THALER, G. T., NORTON, D. P., THEODOROPOULOU, N., HEBARD, A. F., PARK, Y. D., REN, F., KIM, J. and BOATNER, L. A. Wide band gap ferromagnetic semiconductors and oxides. *Journal of Applied Physics*. 2003. Vol. 93, no. 1, p. 1.

[8] SUN, S.-J, YU, Ch. F., HSU, H.-S., CHOU, H., DU, A.-J. Mechanism of ferromagnetism in non-magnetic ion-doped zinc oxides. *Physica Scripta*. 2014. Vol. 89, no. 1, p. 015807.

[9] OBA, F., CHOI, M., TOGO, A., TANAKA, I. Point defects in ZnO: an approach from first principles. *Science and Technology of Advanced Materials*. 2011. Vol. 12, no. 3, p. 034302.

[10] ÖZGÜR, Ü., ALIVOV, Ya. I., LIU, C., TEKE, A., RESHCHIKOV, M. A., DOĞAN, S., AVRUTIN, V., CHO, S.-J. and MORKOÇ, H. A comprehensive review of ZnO materials and devices. *Journal of Applied Physics*. 2005. Vol. 98, no. 4, p. 041301.

[11] REMES, Z., BABCHENKO, O., VARGA, M., STUCHLIK, J., JIRASEK, V., PRAJZLER, V., NEKVINDOVA, P., KROMKA, A. Preparation and optical properties of nanocrystalline diamond coatings for infrared planar waveguides. *Thin Solid Films* [in print]. DOI 10.1016/j.tsf.2016.04.026

[12] PRAJZLER, V., NEKVINDOVÁ, P., VARGA, M., KROMKA, A., REMEŠ, Z. Design of 1x2 wavelength demultiplexer based on multimode interference. *Journal of Optoelectronics and Advanced Materials*. 2014. Vol. 16, no. 11-12, pp. 1226-1231.

[13] KELLY, P.J, ARNELL, R.D. Magnetron sputtering: a review of recent developments and applications. *Vacuum*. 2000. Vol. 56, no. 3, pp. 159-172.

[14] MUSIL, J., BAROCHA, P., VLCEK, J., NAM, K. H., HAN, J. G., Reactive magnetron sputtering of thin films: present status and trends, T*hin Solid Films* vol. 475, 2005, pp. 208- 218

[15] JACKSON, W.B., AMER, N.M., BOCCARA, A.C., FOURNIER, D. Photothermal deflection spectroscopy and detection. *Applied Optics*. 1981. Vol. 20, no. 8, pp. 1333-1344.

[16] TOMPKINS, H. G., MCGAHAN, W. A. *Spectroscopic Ellipsometry and Reflectometry: A User's Guide*. New York : John Wiley & Sons, Inc., 1999.

[17] ASPNES, D. E., THEETEN, J. B., HOTTIER, F. Investigation of effective-medium models of microscopic surface roughness by spectroscopic ellipsometry. *Physical Review B*. 1979. Vol. 20, no. 8, pp. 3292-3302.

[18] SRIKANT, V., CLARKE, D.R. On the optical band gap of zinc oxide. *Journal of Applied Physics*. 1998. Vol. 83, no. 10, pp. 5447-5451.

[19] JIRASEK, V., PRAJZLER, V., REMES, Z. Calculations of nanocrystalline diamond-covered waveguides based on amorphous silicon. In : *NANOCON 2015: 7th International Conference on Nanomaterials - Research and Application*. Ostrava : TANGER LTD, 2015. pp. 39-44. ISBN 978-80-87294-63-5.